

## Measurement of the Electron-Neutron Interaction by the Asymmetrical Scattering of Thermal Neutrons by Noble Gases\*

V. E. KROHN AND G. R. RINGO

*Argonne National Laboratory, Argonne, Illinois*

(Received 4 April 1966; revised manuscript received 5 May 1966)

The electron-neutron interaction has been obtained from measurements of thermal neutron scattering by argon, krypton, and xenon. In terms of the slope of the electric structure factor of the neutron at zero momentum transfer, the values obtained were  $0.0196 \pm 0.0013$  F<sup>2</sup> from Ar,  $0.0197 \pm 0.0007$  F<sup>2</sup> from Kr, and  $0.0190 \pm 0.0005$  F<sup>2</sup> from Xe. The final result is  $0.0193 \pm 0.0004$  F<sup>2</sup>, which corresponds to an electron-neutron scattering length of  $-1.34 \pm 0.03 \times 10^{-16}$  cm and an effective potential of  $-3720 \pm 90$  eV. During the course of the experiment, the neutron-absorption cross sections of krypton and xenon (at 2200 m/sec) were measured by transmission and found to be  $25.0 \pm 0.8$  b and  $25.1 \pm 1.0$  b, respectively. Also, some free-atom thermal-neutron scattering cross sections were measured. The results were  $2.415 \pm 0.010$  b for neon,  $0.647 \pm 0.003$  b for argon,  $7.61 \pm 0.04$  b for krypton,  $4.30 \pm 0.02$  b for xenon,  $73.7 \pm 0.4$  b for <sup>36</sup>Ar,  $1.705 \pm 0.009$  b for <sup>22</sup>Ne, and  $5.1 \pm 0.3$  b for <sup>21</sup>Ne.

### I. INTRODUCTION

THE direct measurement of the electron-neutron interaction<sup>1</sup> with low-energy neutrons currently appears to be the most sensitive available measure of  $[dG_{En}/dq^2]_{q=0}$ , the slope of the electric structure factor of the neutron at zero four-momentum transfer. Along with the charges and magnetic moments of the nucleons and a few parameters derived from high-energy electron-scattering experiments, it provides the main experimental basis for present ideas about nucleon structure. An estimate of the electron-neutron interaction can, of course, be obtained by extrapolating the results of high-energy electron-deuteron scattering experiments to zero four-momentum transfer,<sup>2-7</sup> but this procedure leads to results with relatively large uncertainties.

Some recent arguments based on internal symmetries<sup>8</sup> have suggested that  $G_{En}(q^2) = 0$  for all values of  $q^2$ . However, making use of relativistic invariance, Foldy<sup>9,10</sup> has shown that the anomalous magnetic moment of the neutron implies a contribution of  $+0.021$  F<sup>2</sup> to the electron-neutron interaction. Although other contributions of different physical origin could cancel this, the Foldy effect makes it somewhat plausible that there

should be an electron-neutron interaction of the size that is observed by low-energy neutron scattering.

Three methods involving low-energy neutrons have been used to measure the electron-neutron interaction. All of them in essence are measurements of the scattering length. Havens, Rabi, and Rainwater<sup>11</sup> introduced a method which depends upon the fact that at low neutron energies ( $\lesssim 0.1$  eV) the total scattering cross section of an atom includes an observable term arising from interference between the nucleus and the electrons scattering coherently, while at higher neutron energies ( $\gtrsim 10$  eV) this interference term is almost absent (small atomic scattering factor). The most recent application of this method involved transmission measurements on liquid bismuth<sup>12</sup> and gave the result  $[dG_{En}/dq^2]_{q=0} = 0.0225 \pm 0.0007$  F<sup>2</sup>.

A second method of measurement was used by Hughes, Harvey, Goldberg, and Stafne.<sup>13</sup> It depends upon the fact that the difference in the refractive indices (for neutrons) at an interface between bismuth and liquid oxygen comes largely from the electron-neutron scattering length. Measurements involving the total reflection of low-energy neutrons at such an interface were used to determine this difference, and transmission measurements at higher neutron energies (where, as in the previous method, the electron-neutron interaction is unimportant) were used to determine how much the nuclear scattering lengths of oxygen and bismuth contributed to the difference. The result obtained was  $[dG_{En}/dq^2]_{q=0} = 0.0200 \pm 0.0019$  F<sup>2</sup>.

The third method of measuring the interaction was first employed by Fermi and Marshall<sup>14</sup> and has been used for the work reported here. It depends upon the fact that, in the scattering of thermal neutrons, the interference between the scattering from the nucleus

\* Work performed under the auspices of the U. S. Atomic Energy Commission.

<sup>1</sup> As is usual, the expression "electron-neutron interaction" is used in this paper for the low-energy, spin-independent interaction between the electron and the neutron. This excludes the relatively large interaction between the magnetic dipole moments of the two particles.

<sup>2</sup> B. Bosco, B. Grossetête, and P. Quarati, *Phys. Rev.* **141**, 1441 (1966).

<sup>3</sup> B. Grossetête, D. Drickey, and P. Lehmann, *Phys. Rev.* **141**, 1425 (1966).

<sup>4</sup> L. H. Chan, K. W. Chen, J. R. Dunning, Jr., N. F. Ramsey, J. K. Walker, and Richard Wilson, *Phys. Rev.* **141**, 1298 (1966).

<sup>5</sup> E. B. Hughes, T. A. Griffy, M. R. Yearian, and R. Hofstadter, *Phys. Rev.* **139**, B458 (1965).

<sup>6</sup> F. M. Renard, J. Trần Thanh Vân, and M. Le Bellac, *Nuovo Cimento* **38**, 6268 (1965).

<sup>7</sup> P. Stein, M. Binkley, R. McAllister, A. Suri, and W. Woodward, *Phys. Rev. Letters* **16**, 592 (1966).

<sup>8</sup> K. J. Barnes, P. Carruthers, and F. von Hippel, *Phys. Rev. Letters* **14**, 82 (1965).

<sup>9</sup> L. L. Foldy, *Phys. Rev.* **87**, 693 (1952).

<sup>10</sup> L. L. Foldy, *Rev. Mod. Phys.* **30**, 471 (1958).

<sup>11</sup> W. W. Havens Jr., I. I. Rabi, and L. J. Rainwater, *Phys. Rev.* **72**, 634 (1947).

<sup>12</sup> E. Melkonian, B. M. Rustad, and W. W. Havens Jr., *Phys. Rev.* **114**, 1571 (1959).

<sup>13</sup> D. J. Hughes, J. A. Harvey, M. D. Goldberg, and M. J. Stafne, *Phys. Rev.* **90**, 497 (1953).

<sup>14</sup> E. Fermi and L. Marshall, *Phys. Rev.* **72**, 1139 (1947).

and from the electrons of an atom leads to an asymmetric angular distribution of scattered neutrons in the center-of-mass system. This occurs because the atomic scattering factor (form factor) depends upon the angle of scattering as well as the neutron energy. Monatomic gases at moderate pressures are used in order to avoid diffraction effects, and atoms of zero magnetic moment are selected in order to eliminate the magnetic dipole interaction. In the laboratory system, the motion of the center of mass contributes an asymmetry which is larger than the electron-nucleus interference term in all of the gases. Hence, the basic measurement is a determination of the difference between the observed asymmetry and the asymmetry caused by the motion of the center of mass. Prior to the present experiment,<sup>15</sup> the most precise result obtained by this method ( $0.0202 \pm 0.0041 F^2$ ) was an average of values obtained from studies of krypton and xenon scattering<sup>16</sup> combined with measured values of the coherent scattering lengths of krypton and xenon.<sup>17</sup>

Because the electron-neutron interaction is so small in comparison with the neutron-nucleus interaction, there is always a serious concern that some small effect involving the nuclear interaction may be affecting the measurement in an unknown way. For example, in the measurements involving bismuth a change of 1 part in 1000 in the neutron cross section of bismuth between 0 and 10 eV would change the measured electron-neutron interaction by roughly 10%. In the measurements involving the noble gases, a weak *p*-wave resonance near thermal energy could affect the result. It is thus unusually important to have this measurement made by several methods and on various materials. Accordingly, we decided to repeat the measurement on the noble gases in order to achieve precision comparable to that of the bismuth measurements with each of three gases.

## II. MEASUREMENT OF THE ASYMMETRY

The measurement of the ratio of the number of neutrons scattered through  $45^\circ$  in the laboratory to the number scattered through  $135^\circ$  has proved to be a convenient method of determining the asymmetry,<sup>14,16</sup> and these angles have been retained for the present work. The use of two counters at each angle<sup>16</sup> is of considerable importance in effecting a cancellation of small errors in the alignment of the apparatus and this arrangement has been retained also. The collimation of the incident neutron beam, the cadmium channels within the scattering chamber, and the boron carbide shielding around the counters and chamber were designed to minimize the background, which varied from 2.4% to 14% depending on the collimation of the inci-

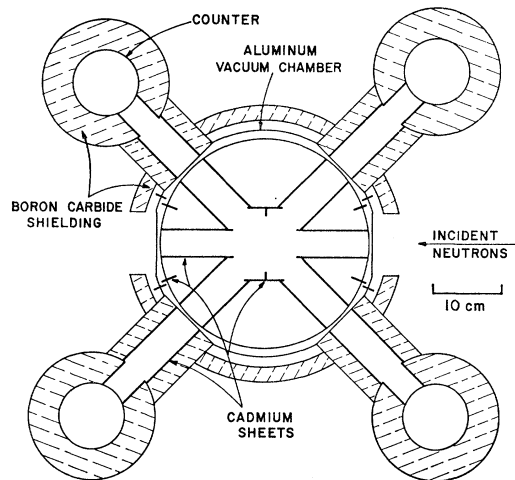


FIG. 1. The scattering chamber used for the measurement of the asymmetry ratios.

dent beam, the gas pressure, and the scattering cross section of the gas being studied. Figure 1 shows some of the details of the scattering chamber.

Two sets of counters containing mixtures of  $^3\text{He}$ , neon, and methane were used.<sup>18</sup> All of the counters had diameters of 8.9 cm but the  $^3\text{He}$  pressure (at  $0^\circ\text{C}$ ) was 0.99 atm in the set used for most of the measurements (the high-efficiency counters) and 0.348 atm in the alternative set (the low-efficiency counters). The dead time of the counting systems was 4.7  $\mu\text{sec}$  and the counting rates varied from 40 000 to 300 000/min. The ionization rate (in air) at the counter positions varied from 50 to 300 mR/h, depending on the arrangement for the collimation of the incident neutron beam. Small adjustments in the positions of the collimators with respect to the face of the reactor shielding ensured that the ionization density was within 10% of the same value in all four counter positions. Measurements showed that a gamma field of 300 mR/h affected the counting rates of the detectors by less than 1 part in  $10^3$ . Since the gamma fields at the counters were balanced to about 20 mR/h and the unbalance was random with respect to the  $45^\circ$  and  $135^\circ$  sets of counters, it seems safe to conclude that the gammas affected the asymmetry measurements by a few parts in  $10^5$  or less.

There was 15 cm of lead between the reactor tank and the neutron collimation system. The opening in the end of the collimator adjacent to this lead was 1.5 cm wide and 17 cm high. The collimating system extended over a distance of 2.1 m. The center of the scattering chamber was 48 cm beyond this. Angles in the vertical plane were restricted by Soller slits (a set of parallel absorbing plates) spaced 3.4 cm apart and extending for 1 m in the section of the collimator embedded in the graphite of the thermal column. The collimation was varied for some of the measurements. This was done by changing

<sup>15</sup> A preliminary report on this experiment was presented by V. E. Krohn and G. R. Ringo, *Phys. Letters* **18**, 297 (1965).

<sup>16</sup> M. Hamermesh, G. R. Ringo, and A. Wattenberg, *Phys. Rev.* **85**, 483 (1952).

<sup>17</sup> M. F. Crouch, V. E. Krohn, and G. R. Ringo, *Phys. Rev.* **102**, 1321 (1956).

<sup>18</sup> V. E. Krohn, *Rev. Sci. Instr.* **35**, 853 (1964).

TABLE I. The limits of angular divergence and beam area for the various experimental arrangements.

Arrangement	Limits of angular divergence		Dimension of beam at center of scattering chamber	
	Vertical (mrad)	Horizontal (mrad)	Full height (cm)	Full width (cm)
Open and stopper <sup>a</sup>	±34	±8.8	17.2	3.1
Narrow	±34	±5.4	15.6	1.3
Soller slit	±23	±8.8	16.1	3.1

<sup>a</sup> Outer limits of stopper arrangement are the same as the open but the central area is removed.

the section of the collimating system at the face of the reactor shielding. The most open section for this last 30 cm of collimation was 13.8 cm high and 2.2 cm wide (the open arrangement). Three other arrangements were available. One provided an opening 12.2 cm high and 0.8 cm wide (the narrow arrangement), another had a 9.5×1.4-cm cadmium plate which intercepted the center of the open beam (the stopper arrangement), and the third was the size of the open arrangement but contained some additional Soller slits which were 30 cm long and spaced 0.7 cm apart (the Soller-slit arrangement). Table I shows the limits of angular divergence and the areas of the beams corresponding to these arrangements.

The openings that admitted scattered neutrons to the counters were 30 cm from the center of the scattering chamber and were 14.6 cm high and 5.2 cm wide. In order to restrict the scattered neutrons to a small range of angles centered on the horizontal plane, horizontal sheets of cadmium were installed, inside and outside the chamber, at the midplane of the channels through which scattered neutrons passed to the counters. In addition, some Soller slits could be placed between the scattering chamber and the counters to provide a closer restriction on the angles of scattered neutrons with respect to the horizontal plane. These slits were 9.5 cm long and were spaced 0.85 cm apart. They were used along with the open collimation of the incident beam. This was called the "slits-after" arrangement.

For each arrangement, geometric corrections (and also the mean cosines of the scattering angles) were determined by numerical calculations. These geometric corrections take account of the divergence and finite width of the incident beam, the attenuation of the incident beam in the scattering gas, and the finite solid angle over which the detectors accepted scattered neutrons.

Xenon, krypton, and argon were used as scattering gases for the measurement of the electron-neutron interaction, and neon was studied to provide a test of the calculation of the effect of the motion of the center of mass.

The procedure followed in taking scattering data was to count for 10 min, rotate the assembly consisting of

the scattering chamber and counters through 180° and count for 20 min (2 counts of 10 min each), then rotate through 180° and count for an additional 10 min (with the counters in their original positions).

After subtraction of the background, two ratios (counts at 45° to counts at 135°) were obtained from each 10-min interval of counting with the 4 counters. The final result from a 40-min run was the geometric mean of eight ratios of this kind. This method of analysis yields a result which is independent of differences in the efficiencies of the 4 counters and is insensitive (to first order) to misalignment of the scattering chamber with respect to the beam.

Background data were obtained before and after groups of about three runs of the type just described. In order to obtain the background data, the scattering gases (except neon) were condensed in a cold finger which was permanently attached to the scattering chamber. Liquid nitrogen was used to condense krypton and xenon while argon was condensed by solid nitrogen produced by pumping on the liquid with a roughing pump. Background data for neon were obtained with the chamber evacuated by pumps before and after groups of about six runs.

Additional runs were made with cadmium in the beam so that the effects of the scattering of epicalcium neutrons by the gases could be subtracted. These runs were made with gas alternately in and out of the chamber. The subtraction of the epicalcium effects changed the measured asymmetry ratio by  $2.1 \times 10^{-3}$  in the case of xenon at the lowest pressure, but the biggest change in the gases other than xenon was  $4.1 \times 10^{-4}$ . The change became smaller at higher xenon pressures and was  $5.4 \times 10^{-4}$  at the highest xenon pressure with the open-collimation arrangement. These effects can be understood in a general way if one notes that there is a strong neutron scattering resonance in <sup>133</sup>Xe at 14.1 eV.

In addition to varying the geometric arrangement and the efficiency of the counters, we used three different gas pressures with xenon and two different pressures with krypton. These measurements were made in order to test for the possible presence of diffraction effects associated with a tendency of gas at moderate pressure to exhibit structure effects similar to those found in liquids.

During the course of the experiment, the chamber was evacuated and filled with clean gas 20 times so that each filling (combination of pressure and scattering gas) was repeated at least once. Argon and neon were discarded after being used but krypton and xenon were saved. Before each filling, the gas was purified (or repurified) by passage over titanium powder held at 925°C.

Table II summarizes the results of the asymmetry measurements. In addition, a number of runs were made to test for possible sources of systematic error. These included runs with large masses of material adjacent to one of the counter shields, runs with 50-G magnetic fields (of different orientations) at 3 of

TABLE II. Summary of asymmetry determinations. The electron-neutron effect (column 9) is obtained by dividing the measured asymmetry ratio (column 5) by the geometric correction and the center-of-mass asymmetry ratio (columns 6 and 8) and then subtracting 1.0 and multiplying by  $10^6$ . The uncertainties given in column 9 are those associated with the measured ratios only.

(1) Gas	(2) Arrangement	(3) Counter efficiency	(4) Gas pressure (atm)	(5) Measured asymmetry ratio	(6) Geometric correction	(7) Mean $ \cos\theta $	(8) C.m. asymmetry ratio	(9) $e-n$ effect (parts in $10^6$ )
Ne	open	high	1.68	1.13307	1.00041	0.7049	1.13457	-173±40
Ar	open	high	1.65	1.06598	1.00039	0.7049	1.06997	-412±17
Kr	narrow	high	1.06	1.02894	1.00047	0.7054	1.03191	-335±17
Kr	slit	high	1.06	1.02883	1.00050	0.7048	1.03189	-348±14
Kr	stopper	high	1.06	1.02899	1.00072	0.7041	1.03189	-353±14
Kr	slit-after	high	1.06	1.02946	1.00062	0.7107	1.03221	-328±17
Kr	open	high	1.06	1.02932	1.00066	0.7049	1.03194	-320±10
Kr	open	high	0.33	1.02926	1.00046	0.7049	1.03189	-301±14
Kr	open	low	1.06	1.02859	1.00068	0.7049	1.03104	-306±9
Xe	slit	high	1.30	1.01544	1.00053	0.7048	1.02039	-538±15
Xe	open	high	1.30	1.01588	1.00069	0.7049	1.02039	-511±10
Xe	open	high	0.88	1.01575	1.00058	0.7049	1.02037	-511±14
Xe	open	high	0.39	1.01584	1.00047	0.7049	1.02039	-493±11
Xe	open	low	1.18	1.01536	1.00071	0.7049	1.01987	-513±11

the counter positions, runs with the scattering chamber rotated through an angle that differed from  $180^\circ$  by a great deal more than the uncertainty involved in setting the angle, runs with the center of the scattering chamber off the center of the beam by an amount much larger than the uncertainty in the actual alignment of these centers, runs made after krypton had been contaminated with large quantities of several hydrocarbons prior to being repurified, and runs to look for an observable effect from material that accumulated in the chamber during 16 h of outgassing. None of these runs indicated that the results were subject to systematic errors.

Since contaminating a scattering gas with about 1 part per million (i.e., about a micron of pressure) of a hydrocarbon which could stay with the noble gas during the background and scattering runs would cause a significant systematic error in the measurements, special tests (in addition to those already mentioned) were made to show that such contamination was not occurring. First, it was demonstrated that the total leakage and outgassing rate of the chamber was about  $7 \mu$  per day and that less than  $0.3 \mu$  of this could be trapped by liquid nitrogen. Although this test suggested that contamination during a series of runs was not a serious problem, an additional test was made by analyzing the data to see if the asymmetries tended to change with time after filling the chamber with a clean scattering gas. No significant change was found.

### III. CALCULATION OF THE ASYMMETRY CAUSED BY MOTION OF THE CENTER OF MASS

In the scattering experiments on the noble gases, the center of mass of the neutron and target atom has an average forward velocity (because of the neutron velocity). The consequent asymmetry in the scattering as measured in the laboratory system is actually larger

than that coming from the electron-neutron interaction. It is a function of the efficiency of the neutron counters, the neutron velocity spectrum, and the mass and temperature of the target atoms (which are assumed to have a Maxwellian velocity distribution). Fortunately, the effect of the center-of-mass motion can be calculated by a relatively straightforward classical calculation.

Consider the probability  $P(\mathbf{v})$  that a neutron with initial velocity  $\mathbf{v}_0$  will have a final velocity  $\mathbf{v}$ , given that it is scattered from an atom with initial velocity  $\mathbf{V}$  (all velocities being in the laboratory system). This probability can be obtained by starting with the center-of-mass system in which the distribution is isotropic with  $v_0' = v'$  and in which

$$P(\mathbf{v}')d\mathbf{v}' = [1/(2\pi v_0')] \delta(v_0'^2 - v'^2) d\mathbf{v}', \quad (1)$$

where  $\mathbf{v}_0'$  and  $\mathbf{v}'$  are the initial- and final-neutron velocities in the center-of-mass system and  $\delta$  is the Dirac delta function. When this is transformed to the laboratory system by replacing  $\mathbf{v}_0'$  and  $\mathbf{v}'$  by their expressions in terms of the laboratory velocities and noting that  $d\mathbf{v}' = d\mathbf{v}$ , the result is

$$P(\mathbf{v})d\mathbf{v} = \frac{A+1}{2\pi A |\mathbf{v}_0 - \mathbf{V}|} \delta \left\{ \left( \frac{A}{A+1} \right)^2 (\mathbf{v}_0 - \mathbf{V})^2 - \left[ \mathbf{v} - \frac{1}{A+1} (\mathbf{v}_0 + A\mathbf{V}) \right]^2 \right\} d\mathbf{v}, \quad (2)$$

where  $A$  is the ratio of the mass of the scattering atom to the neutron mass.

The probability of a scattering event occurring in the first place with initial velocities  $\mathbf{v}_0$  and  $\mathbf{V}$  is (for unit length of incident neutron path and one target atom per unit volume)

$$P(\mathbf{v}_0, \mathbf{V}) d\mathbf{v}_0 d\mathbf{V} = N(v_0) M(\mathbf{V}) \sigma_s(|\mathbf{v}_0 - \mathbf{V}|/v_0) d\mathbf{v}_0 d\mathbf{V}, \quad (3)$$

where  $N(v_0)$  is the normalized distribution of the magnitudes of the incident neutron velocities,  $M(\mathbf{V})$  is the Maxwellian distribution of target-gas velocities,  $\sigma_s$  is the (free-atom) neutron scattering cross section of the scattering gas, and  $|\mathbf{v}_0 - \mathbf{V}|$  is the magnitude of the relative velocity.

The next step is to rearrange the terms in the delta function, take the product of Eqs. (2) and (3), and integrate over the velocity distribution of target-gas atoms. The direction of  $\mathbf{v}_0 - \mathbf{v}$  is chosen as the polar axis and  $\psi$  is used to designate the polar angle. The integration over the azimuthal angle, because of the polar axis selected, simply yields a factor of  $2\pi$ . Hence, a scattering event in which the initial neutron speed is  $v_0$  and the final neutron velocity is  $\mathbf{v}$  occurs with the probability

$$P(v_0, \mathbf{v}) dv_0 d\mathbf{v} = \frac{\sigma_s N(v_0) (A+1)}{4\pi A v_0} dv dv_0 \int_0^\infty M(V) \times \int_0^\pi \delta \left[ \frac{2A}{A+1} |\mathbf{v} - \mathbf{v}_0| V \cos \psi - \left( v^2 - v_0^2 \frac{A-1}{A+1} - \frac{2\mathbf{v} \cdot \mathbf{v}_0}{A+1} \right) \right] \sin \psi d\psi dV. \quad (4)$$

The differential of the argument of the delta function is  $-2A(A+1)^{-1} |\mathbf{v} - \mathbf{v}_0| V \sin \psi d\psi$  and the integration over  $\psi$  will include a root of the argument of the delta function if

$$V \geq \left| v^2 - v_0^2 \frac{A-1}{A+1} - \frac{2\mathbf{v} \cdot \mathbf{v}_0}{A+1} \right| / \left( \frac{2A}{A+1} |\mathbf{v} - \mathbf{v}_0| \right). \quad (5)$$

This expression becomes the lower limit for the integration with respect to  $V$ . The latter integration is performed analytically and the result is multiplied by the counting efficiency  $\epsilon(v)$  and integrated over the magnitudes of the incident and final neutron velocities. The resulting probability (for one target atom per unit volume and one unit length of incident neutron path) of counting a neutron at angle  $\theta$  with respect to the incident neutron direction is

$$P(\theta) d\Omega = \frac{\sigma_s (A+1)^2 d\Omega}{4A^2 \pi^{3/2} B_0} \int_0^\infty N(v_0) \times \int_0^\infty \frac{\epsilon(v) \mathcal{F}(v, v_0, \theta) v^2 dv dv_0}{v_0 (v^2 + v_0^2 - 2vv_0 \cos \theta)^{1/2}}, \quad (6)$$

where

$$\mathcal{F}(v, v_0, \theta) = \exp \left\{ - \left( v^2 - v_0^2 \frac{A-1}{A+1} - \frac{2vv_0 \cos \theta}{A+1} \right)^2 / \left[ \frac{4A^2}{(A+1)^2} B_0^2 (v^2 + v_0^2 - 2vv_0 \cos \theta) \right] \right\},$$

$d\Omega$  is the differential solid angle for the scattered

neutron,  $\theta$  is the angle from the incident to the final neutron direction, and  $B_0 = (2kT_g/AM)^{1/2}$  with  $T_g$  the temperature of the target gas and  $M$  the neutron mass.

Since approximate methods of evaluating Eq. (6) by expanding in powers of  $1/A$  were not adequate for our purposes, the integrations for the present measurements were performed on a computer. The results are given in Table II (column 8). The neutron spectrum  $N(v_0)$  used for these integrations was measured with a slow chopper and corrected for attenuation in the scattering gases prior to the scattering event and for temperature variations of the moderator in the reactor. The expression used for the counting efficiency was

$$\epsilon(v) = (1 - e^{-L/v}) e^{-K/v} \quad (7)$$

with  $L$  proportional to the average length of the neutron trajectories through the counters. An additional computation was performed to show that the use of an average  $L$  was adequate for our purposes. The factor  $e^{-K/v}$  is the absorption of neutrons between the scattering event and the counter.

In order to do an exact calculation for an element, the integral of Eq. (6) should be evaluated for each isotope and the results weighted with the isotopic scattering cross sections and isotopic abundances. However, the asymmetries are approximately proportional to  $1/A$  and in each case it was satisfactory to do a single calculation with the value of  $A$  given by

$$A = \frac{\sigma_s}{\sum n_i \sigma_i / A_i}, \quad (8)$$

where the  $n_i$  are the abundances and the  $\sigma_i$  the scattering cross sections of the isotopes, and the  $A_i$  are ratios of the isotopic masses to the neutron mass. Measurements of the  $\sigma_s$  and  $\sigma_i$  are discussed in the next section and the values of  $A$  calculated for use with each scattering gas are given in Table III.

The values of  $\cos \theta$  used in the computer integration of Eq. (6) differed slightly from those for the nominal angles,  $45^\circ$  and  $135^\circ$ . The values used (Table II) were obtained by numerical integration. The numerical calculations included consideration of angles out of the

TABLE III. Quantities needed for the determination of the final results.

	Ne	Ar	Kr	Xe
$A$ [from Eq. (8)]	19.938	37.998	83.04	129.99
$1+\delta$	1.0 <sup>a</sup>	1.000	1.003	1.001
$\Delta F$	2.3 <sup>a</sup>	4.34	9.87 <sup>b</sup>	13.91 <sup>b</sup>
$\sigma_s$ (free atom) (b)	2.415	0.647	7.61	4.30
$\sigma_s$ (bound nucleus) (b)	2.67	0.686	7.84	4.41
$a$ (bound nucleus) (F)	4.60	1.909	7.44	4.87

<sup>a</sup> Estimated.

<sup>b</sup> These values of  $\Delta F$  are appropriate for use with the weighted mean of the electron-neutron effect (column 9 of Table II) for the particular gas.  $\Delta F$  actually depends on  $|\cos \theta|$  and, in addition, it is smaller for the low-efficiency counters than for the high-efficiency ones, the difference being 1.2% with xenon and 1.6% with krypton.

horizontal plane. Special calculations showed that the use of the mean cosines in evaluating Eq. (6) gave results which were adequately accurate for our purposes.

#### IV. MEASUREMENT OF SCATTERING CROSS SECTIONS

A special experimental arrangement was assembled for the measurement of the thermal-neutron scattering cross sections of the noble gases and their separated isotopes. The measurements were made relative to the  $2.415 \pm 0.010$  b free-atom scattering cross section of natural neon which was obtained from transmission measurements.

The aluminum scattering chamber for these measurements was 3.3 cm in diameter and 14 cm long and had concave end windows 0.013 cm thick. The interior of the 0.10-cm side wall of the scattering chamber was plated with 0.025 cm of cadmium except for the central 5 cm of length. Neutrons scattered out of the central 5 cm of the chamber were observed by two  $^3\text{He}$  counters<sup>18</sup> well shielded from stray neutrons by boron carbon powder in metal cans.

The absolute pressures of the scattering gases ranged from 0.18 to 0.99 atm. The amount of scatterer was determined from the Van der Waals equation of state by use of pressures measured on a large Bourdon gauge certified to be accurate to  $\pm 0.0005$  atm. Special numerical integrations of Eq. (6) for angles near  $90^\circ$  were used to correct the results for the effects of the motion of the center of mass and the usual corrections for the dead time of the counters were made. The contribution of episcadmium neutrons was measured in each case and subtracted.

Relatively pure samples of  $^{36}\text{Ar}$  and  $^{22}\text{Ne}$  were available so that the cross sections of these isotopes could be measured to the same accuracy as the cross sections of the natural elements, that is, to  $\pm 0.3\%$  relative to natural neon. The results for the free-atom thermal-neutron scattering cross sections of these isotopes were  $73.7 \pm 0.4$  b for  $^{36}\text{Ar}$  and  $1.705 \pm 0.009$  b for  $^{22}\text{Ne}$ . The results obtained for the free-atom scattering cross sections of the natural elements were  $0.647 \pm 0.003$  b for argon,  $7.61 \pm 0.04$  b for krypton, and  $4.30 \pm 0.02$  b for xenon. Our results for the natural elements including neon are in agreement with the results obtained at Saclay,<sup>19</sup> but they appear to be more precise.

Our sample of  $^{21}\text{Ne}$  contained only 11.2% of the isotope of interest. The value obtained for the free-atom scattering cross section of  $^{21}\text{Ne}$  was  $5.1 \pm 0.3$  b. The result deduced for the scattering cross section of  $^{38}\text{Ar}$  from measurements with a sample containing 17.75%  $^{38}\text{Ar}$  and 35.05%  $^{36}\text{Ar}$  was  $1.5 \pm 1.5$  b.

The results obtained with mixtures of krypton and xenon isotopes (Tables IV and V) did not permit determination of the cross section of each isotope but they

were of considerable value in estimating the  $A$ 's (Table III).

#### V. THE INTERFERENCE BETWEEN NUCLEAR AND ELECTRONIC SCATTERING

The differential cross section for the scattering of neutrons by the atoms of a monatomic gas may be written

$$d\sigma/d\Omega = \sum n_i [a_i + bF(\theta)]^2 = \sum n_i [a_i^2 + 2a_i bF(\theta) + b^2 F^2(\theta)], \quad (9)$$

where the  $a_i$  are the nuclear scattering lengths of the isotopes,  $b$  is the electron-neutron scattering length, and  $F(\theta)$  is the atomic scattering factor (form factor) of the electron distribution and includes the factor  $Z$  which is sometimes written separately. The first term on the right is the differential nuclear-scattering cross section of the element, the second is the electron-nucleus interference term, and the third gives the scattering by the electrons alone and is almost negligible. The sum  $\sum n_i a_i$  in the second term is the coherent nuclear scattering length  $a$  of the element. To second order in  $b/a$ , the ratio  $R = \sigma(45^\circ)/\sigma(135^\circ)$  expected from isotropic nuclear scattering in combination with effects of the electron-neutron interaction is seen to be

$$R = 1 + (8\pi ab \Delta F / \sigma_s)(1 + \delta), \quad (10)$$

where  $\Delta F = \langle F(45^\circ) - F(135^\circ) \rangle_{\text{av}}$  and

$$\delta = \frac{b}{2a\Delta F} \langle F^2(45^\circ) - F^2(135^\circ) \rangle_{\text{av}} - \frac{8\pi ab}{\sigma_s} \langle F(135^\circ) \rangle_{\text{av}}.$$

This  $R$  is to be equated with the quotient obtained by dividing the ratio measured in the laboratory by the ratio that would arise (from an isotropic distribution in the center-of-mass system) as a result of the motion of the center of mass.

Since the terms that contribute to  $\delta$  are between 0.003 and 0.011, a very crude evaluation is sufficient. On the other hand, it is essential that good values of the coherent scattering length  $a$ , the scattering cross section  $\sigma_s$ , and the effective scattering factor  $\Delta F$  be obtained if a good measurement of  $b$  is to be achieved.

TABLE IV. Neutron-scattering cross sections for some mixtures of krypton isotopes.

Mass number	78	80	82	83	84	86	$\frac{\sigma_s(\text{sample})}{\sigma_s(\text{natural Kr})}$
	Isotopic concentration (%)						
Sample No. 1	6.47	18.71	27.43	13.25	32.11	2.03	1.000
2	0.75	3.91	15.23	12.91	55.04	12.16	1.005
3		0.02	1.02	3.23	44.10	51.63	0.960
4			0.14	0.89	22.84	76.13	0.959
Natural Kr	0.35	2.27	11.56	11.55	56.90	17.37	1

<sup>19</sup> R. Genin, H. Beil, C. Signarbieux, P. Carlos, R. Joly, and M. Ribrag, J. Phys. Radium **24**, 21 (1963).

TABLE V. Neutron-scattering cross sections for some mixtures of xenon isotopes.

Mass number	124	126	128	129	130	131	132	134	136	$\frac{\sigma_s(\text{sample})}{\sigma_s(\text{natural Xe})}$
Sample No. 1	5.1	1.7	11.3	62.1	4.3	9.7	5.4	0.4		1.15
2						25.47	30.13	27.18	17.22	0.939
3						3.58	7.36	24.54	64.25	1.015
Natural Xe	0.09	0.09	1.92	26.44	4.08	21.18	26.89	10.44	8.87	1

## VI. THE ATOMIC SCATTERING FACTOR

Since  $F(\theta)$  depends on the neutron velocity, its use in the present experiment requires taking averages over the neutron spectrum with a weighting proportional to the counter efficiency, the result being

$$\langle F(\theta) \rangle_{\text{av}} = \frac{\int F(\theta) N(v_0) \epsilon(v_0) dv_0}{\int N(v_0) \epsilon(v_0) dv_0} \quad (11)$$

with a similar expression for  $\langle F^2(\theta) \rangle_{\text{av}}$ . Values for  $\Delta F$  (Table III) were obtained by numerical evaluation of Eq. (11) with the aid of tables of atomic scattering factors calculated by the Hartree-Fock method of self-consistent fields.<sup>20</sup> Parts of each of these tables have been confirmed by x-ray measurements.<sup>21</sup>

The velocities associated with the thermal motion and the recoil of the target atoms are more important in neutron scattering than in x-ray scattering because they may cause a significant change in the neutron wavelength. However, it was determined that the effect of this on the scattering factor can be neglected.

## VII. THE COHERENT SCATTERING LENGTHS

For neon and argon the coherent scattering lengths were calculated from the scattering cross sections of the isotopes. The calculation took advantage of Henshaw's evidence<sup>22</sup> that the <sup>36</sup>Ar and <sup>40</sup>Ar scattering lengths have the same sign. Positive scattering lengths were assumed for all of the argon and neon isotopes.

Two methods were available for the determination of the coherent scattering length on xenon. First, the value obtained relative to fluorine<sup>23</sup> from neutron diffraction by XeF<sub>4</sub> was normalized to a value of  $5.60 \pm 0.10$  F for

fluorine<sup>24,25</sup> and corrected for the contribution of the electron-neutron interaction. The result was  $4.89 \pm 0.10$  F for xenon.

The second method for xenon, and the only method available for krypton, was to use the results obtained by the critical reflection of neutrons from surfaces of the liquefied gases.<sup>17</sup> These results were corrected to take account of a number of new measurements. First, the correction for attenuation of the neutron beam in the gas above the liquid surfaces was modified to conform to the absorption cross sections measured at Saclay<sup>19</sup> and confirmed by some transmission measurements made during the course of our asymmetry measurements. In the latter, we found  $25.0 \pm 0.8$  b and  $25.1 \pm 1.0$  b for the absorption cross sections of krypton and xenon, respectively, at 2200 m/sec. Second, measurements of the neutron spectrum indicate that the assumption of a Maxwellian spectrum was satisfactory in the case of the krypton data but that the intensity of neutron reflection from xenon and from the associated mixture of ordinary and heavy water would be expected to vary as the  $\frac{5}{2}$  power instead of the square of the scattering lengths. The xenon result was corrected for this. Third, the results were adjusted for new values of the scattering lengths of the materials in the water mixtures used for comparisons. The current values are  $6.21 \pm 0.05$  F for deuterium,<sup>26</sup> 5.80 F for oxygen,<sup>24</sup> and  $-3.74$  F for hydrogen.<sup>27</sup>

The new result for deuterium represents a serious departure from the previously accepted value<sup>24,25</sup>  $6.7 \pm 0.08$  F. This accounts for most of the difference between the electron-neutron interaction reported here and the values given in our preliminary report.<sup>15</sup> The new result for the deuterium scattering length is consistent with the result that can be calculated from the incoherent scattering cross section of the deuterium<sup>28</sup> and the total free-atom cross section of the deuterium.<sup>29</sup>

After the three corrections just described, the mirror-reflection results for the coherent scattering lengths of

<sup>20</sup> For argon: J. Berghuis, I. M. Haanappel, M. Potters, B. O. Loopstra, C. H. MacGillavry, and A. L. Veenendaal, *Acta Cryst.* **8**, 478 (1955). For krypton: results of A. J. Freeman and R. E. Watson, in *International Tables for X-Ray Crystallography*, edited by C. H. MacGillavry and G. D. Rieck (Kynoch Press, Birmingham, England, 1962), Vol. III. For xenon: A. J. Freeman and R. E. Watson (unpublished).

<sup>21</sup> D. R. Chipman and L. D. Jennings, *Phys. Rev.* **132**, 728 (1963).

<sup>22</sup> D. G. Henshaw, *Phys. Rev.* **105**, 976 (1957).

<sup>23</sup> J. H. Burns, P. A. Agron, and H. A. Levy, in *Noble Gas Compounds*, edited by H. H. Hyman (The University of Chicago Press, Chicago, Illinois, 1963), p. 211.

<sup>24</sup> W. Bartolini, R. E. Donaldson, and L. Passell, *Bull. Am. Phys. Soc.* **8**, 477 (1963).

<sup>25</sup> *Neutron Cross Sections*, edited by J. R. Stehn, M. D. Goldberg, B. A. Magurno, and R. Wiener-Chasman (U. S. Department of Commerce, Washington 25, D. C., 1964), BNL-325, 2nd ed., Suppl. No. 2, Vol. I.

<sup>26</sup> W. Bartolini, R. E. Donaldson, and L. Passell (unpublished).

<sup>27</sup> W. C. Dickinson, L. Passell, and O. Halpern, *Phys. Rev.* **126**, 632 (1963).

<sup>28</sup> W. Gissler, *Z. Krist.* **118**, 149 (1963).

<sup>29</sup> R. G. Fluharty, *Ref. 25*, p. 1-comp-1.

TABLE VI. Contributions (%) to the uncertainties in the results.

	Neon result	Argon result	Krypton result	Xenon result	Final result <sup>a</sup> (Ar+Kr+Xe)
Measurement of asymmetry	28.6 <sup>a</sup>	5.4	2.1	1.4	1.2
Effect of uncertainties in spectrum and angles on calculated c.m. asymmetry	21.4 <sup>a</sup>	3.6	1.5	0.8	1.2
Effect of uncertainty in $A$ [Eq. (8)] on c.m. asymmetry		0.1	0.2	0.2	0.2
Absolute neon scattering cross section		0.2 <sup>b</sup>	0.4	0.4	0.4
Relative scattering cross-section measurements		0.3	0.3	0.3	0.2
Coherent scattering length, $a$		0.2 <sup>b</sup>	2.0	1.6	1.2
Scattering factor, $\Delta F$		1.0	1.0	1.0	0.8
Resultant uncertainty	35.6 <sup>a</sup>	6.6	3.5	2.5	2.3 <sup>c</sup>

<sup>a</sup> Expressed as percent of the final result obtained from the other three gases.

<sup>b</sup> In addition to the 0.2% uncertainty listed for the coherent scattering length of argon, there is a 0.2% uncertainty which causes the result from argon to depend less on the absolute neon cross section.

<sup>c</sup> It should be noted that the correlation between some of the uncertainties has been taken into account.

krypton and xenon became  $7.44 \pm 0.15$  F and  $4.85 \pm 0.13$  F, respectively. The xenon result is in excellent agreement with the result obtained from neutron diffraction by  $\text{XeF}_4$ .

### VIII. RESULTS

Values of the electron-neutron scattering length were obtained by substituting the appropriate quantities from Table III into the second term of Eq. (10) and equating this term to the electron-neutron effect given in column 9 of Table II. We elected to use the bound-atom values of the nuclear scattering lengths and scattering cross sections so that we would obtain values of the electron-neutron scattering length corresponding to electrons bound to an infinite mass. This is equivalent to using the free-atom values and then correcting the results for the fact that they apply to electrons bound to atoms of finite mass.

The uncertainties given in Table II (column 9) were obtained from the scatter of the data among the different runs for a given combination of gas, pressure, geometric arrangement, and counter efficiency or from the counting statistics, depending on which approach gave the larger uncertainty. However, it was found that the scatter of the results among different lines of Table II for a given gas (with different geometric arrangements, counters, and pressures) indicated that the uncertainties given in column 9 of the table ought to be increased by a factor of 1.47 for krypton and 1.33 for xenon if this additional scatter was a random effect not associated with anything systematic. This seemed likely. Hence the uncertainties in the final results from krypton and xenon were increased by the aforemen-

tioned factors and the uncertainty associated with the argon result was increased (somewhat arbitrarily) by a factor of 1.33. The final uncertainties associated with the measured asymmetries are given on the first line of Table VI. Additional entries in Table VI give the uncertainties associated with the other factors involved in the measurements and Table VII gives a summary of the results.

### IX. DISCUSSION

The agreement between the results from the three gases (Ar, Kr, and Xe) suggests that the final result has not been seriously affected by any possible weak  $p$ -wave resonance in one of the noble gas isotopes. The neon measurements provide a check of the procedures for calculating the asymmetries associated with the motion of the center of mass. This check is of greater significance than it would seem to be on a basis of the large uncertainty in the neon result for the electron-neutron interaction.

The possibility that a neutron might experience a significant magnetic interaction with a noble gas atom as a result of an induced magnetic moment was considered by Fermi and Marshall.<sup>14</sup> They also considered the effect of the apparent magnetic field that appears in the reference frame of the neutron as a result of the moving nuclear charge of the atom (the effect now known as Schwinger scattering). These effects can still be neglected at the present level of precision.

The use of the measured spectrum in the calculation of the asymmetry associated with the motion of the center of mass and the inclusion of the effect of the uncertainties in the spectrum in estimating the uncertainty in the final result takes care of the objections of Halpern and Hsu.<sup>30,31</sup>

TABLE VII. Summary of results. The second column gives the slope of the electric structure factor of the neutron, the third gives the electron-neutron scattering length, and the fourth indicates the effective potential  $V_0$  that would account for this scattering length if it were effective over a sphere having a radius equal to the classical radius of the electron.

Gas	$[dG_{En}/dq^2]_{q=0}$ (F <sup>2</sup> )	<sup>b</sup> (10 <sup>-16</sup> cm)	$V_0$ (eV)	Statistical weight <sup>b</sup>
Neon	0.025 $\pm$ 0.007 <sup>a</sup>	-1.7 $\pm$ 0.5 <sup>a</sup>	-4800 $\pm$ 1300 <sup>a</sup>	0
Argon	0.0196 $\pm$ 0.0013	-1.36 $\pm$ 0.09	-3780 $\pm$ 250	0.13
Krypton	0.0197 $\pm$ 0.0007	-1.37 $\pm$ 0.05	-3800 $\pm$ 130	0.30
Xenon	0.0190 $\pm$ 0.0005	-1.32 $\pm$ 0.03	-3670 $\pm$ 90	0.57
Weighted mean	0.0193 $\pm$ 0.0004	-1.34 $\pm$ 0.03	-3720 $\pm$ 90	

<sup>a</sup> The neon results are considered only as a check on the procedure and the input data for calculating the center-of-mass asymmetry ratios.

<sup>b</sup> The fact that some of the uncertainties are correlated has been considered in calculating the statistical weights.

<sup>30</sup> O. Halpern and C. P. Hsu, Phys. Rev. **87**, 519 (1952).

<sup>31</sup> O. Halpern, Phys. Rev. **133**, B579 (1964).



Our result disagrees with the bismuth transmission result of Melkonian, Rustad, and Havens.<sup>12</sup> The mirror-reflection measurement<sup>13</sup> is in somewhat better agreement with our result than with the transmission result but it is not as precise as the other results. It is to be hoped that work now underway with the transmission method<sup>22</sup> on bismuth and <sup>208</sup>Pb and the mirror-reflection method<sup>23,24</sup> on bismuth will help to resolve this discrepancy.

<sup>22</sup> R. E. Coté, Argonne National Laboratory (private communication).

<sup>23</sup> W. Triftshäuser, Z. Physik **186**, 23 (1965).

<sup>24</sup> L. Koester, Technische Hochschule, Munich (private communication).

## ACKNOWLEDGMENTS

It is a pleasure to express our gratitude to J. M. Peregrin for his assistance during the entire course of this work, to K. C. Ruzich and Dr. R. E. Coté for help with the measurement of the neutron spectrum, to Dr. M. F. Crouch and Dr. G. L. Squires for their help in the early stages of the experiment, to Dr. F. Chilton, Dr. L. L. Foldy, Dr. F. T. Hagemann, Dr. M. Hamer-mesh, Dr. J. E. Robinson, and Dr. K. S. Singwi for valuable consultations, and to Dr. A. J. Freeman, Dr. R. E. Watson, Dr. W. Bartolini, Dr. R. E. Donaldson, and Dr. L. Passell for giving us unpublished results of their work.

## $\pi^-p$ Interactions at 460 MeV\*

C. P. POIRIER,† C. A. TILGER,‡ E. D. ALYEA, JR., H. J. MARTIN, JR., J. I. RHODE,§  
AND J. H. SCANDRETT

Indiana University, Bloomington, Indiana

(Received 8 April 1966)

A total of 1589 two-prong events were observed in an exposure of the Brookhaven National Laboratory 14-in. bubble chamber at the Cosmotron. The fit to the elastic angular distribution requires terms through  $\cos^4\theta_{c.m.}$ . The ratio of the inelastic cross sections  $\sigma(\pi^-p \rightarrow \pi^- \pi^+ n) / \sigma(\pi^-p \rightarrow \pi^- \pi^0 p)$  is  $3.75 \pm 0.46$ . The  $\pi^-p \rightarrow \pi^- \pi^+ n$  reaction is dominated by formation of the  $\pi^- n$  isobar and an enhancement in the di-pion mass spectrum previously reported by Kirz. The  $\pi^-p \rightarrow \pi^- \pi^0 p$  reaction shows no structure in the effective-mass spectra.

THREE prominent peaks dominate the  $\pi^-p$  total cross section below 1000 MeV. The first is the well-known (3,3) resonance near 200 MeV while the other two are isospin  $T = \frac{1}{2}$  peaks at 610 and 870 MeV. Recently, Bareyre *et al.*<sup>1</sup> examined the energy dependences of the elastic and inelastic  $\pi^-p$  cross sections from 300 to 700 MeV and suggest the possibility of a broad  $T = \frac{1}{2}$  resonance centered near 430 MeV. A discussion of this enhancement (which appears as a shoulder rather than a peak in the elastic cross section) by Dalitz and Moorhouse<sup>2</sup> emphasizes the complexity of the situation when inelastic processes are important and the difficulty of arriving at an unambiguous interpretation of such an enhancement.

The most important feature of inelastic processes in  $\pi^-p$  interactions below 700 MeV is a peaking in the di-

pion effective mass for the  $\pi^-p \rightarrow \pi^+ \pi^- n$  reaction.<sup>3</sup> This enhancement, near the upper kinematical limit of the di-pion spectrum, shifts upward with increasing beam energy and continues to persist over a wide range of incident energies. The reasons for this anomalous behavior are not known, but it does appear to be responsible for the initial importance of inelastic processes in  $\pi^-p$  interactions.

In this experiment we report the results of a study of elastic and inelastic  $\pi^-p$  interactions at 460 MeV. The elastic angular distribution is presented and data on single-pion production are displayed. The importance of isobar formation in these reactions is discussed.

## I. EXPERIMENTAL PROCEDURE

An exposure of 25 000 pictures was taken with the BNL 14-in. hydrogen bubble chamber placed in a negative pion beam at the Cosmotron. The magnetic field at the center of the chamber was 17 290 G. There were 10 to 15 beam tracks in each picture.

Negative pions were produced by bombardment of an internal target in the south straight section of the

\* Supported in part by the National Science Foundation.

† Now at Aerospace Research Laboratory, Wright-Patterson Air Force Base, Ohio.

‡ Now at Physics Department, St. Louis University, St. Louis, Missouri.

§ Now at Iowa State University, Ames, Iowa.

<sup>1</sup> P. Bareyre, C. Bricman, G. Valladas, G. Villet, J. Bizard, and J. Sequinot, Phys. Letters **8**, 137 (1964).

<sup>2</sup> R. H. Dalitz and R. G. Moorhouse, Phys. Letters **14**, 159 (1965).

<sup>3</sup> J. Kirz, J. Schwartz, and R. D. Tripp, Phys. Rev. **130**, 2481 (1963).